Effective pairing interaction in a system with an incipient band

T. A. Maier, V. Mishra, G. Balduzzi, and D. J. Scalapino

Phys. Rev. B **99**, 140504 — Published 15 April 2019

DOI: 10.1103/PhysRevB.99.140504

Effective pairing interaction in a system with an incipient band

T. A. Maier,[1] V. Mishra,[1] G. Balduzzi,[2] and D. J. Scalapino[3]

[1] *Computational Sciences and Engineering Division and Center for Nanophase Materials Sciences, Oak Ridge National Laboratory, Oak Ridge, Tennessee 37831-6164, USA*

[2] *Institute for Theoretical Physics, ETH Zurich, 8093 Zurich, Switzerland*

[3] *Department of Physics, University of California, Santa Barbara, CA 93106-9530, USA*

(Dated: April 2, 2019)

The nature and mechanism of superconductivity in the extremely electron-doped FeSe based superconductors remains an outstanding problem. In these systems, the hole-like band has moved below the Fermi energy, and various spin-fluctuation theories involving pairing between states near the electron Fermi surface and states of this incipient band have been proposed. Here, using a non-perturbative dynamic cluster quantum Monte Carlo calculation for a bilayer Hubbard model, we show how spin-fluctuation scattering involving intermediate virtual states of the incipient band leads to an effective pairing interaction for the electrons on the remaining Fermi surface. The key feature of this interaction is that it is retarded due to the incipient nature of the hole band and the dynamics of the spin-fluctuation interaction. This allows the pairs to avoid the instantaneous repulsive Coulomb interaction and leads to a frequency dependence of the gap which should be observable in tunneling experiments. Our work provides a new perspective for the pairing mechanism in systems with an incipient band that can be tested in future experiments.

The proposal that spin-fluctuation scattering of pairs between the electron and hole Fermi surfaces of the Fe-based superconductors provides the pairing mechanism in these materials is challenged [1] by the occurrence of superconductivity in FeSe monolayers on STO [2–4], and K and Li FeSe intercalates [5–9]. In these materials the hole band near Γ is submerged below the Fermi level leaving only an electron-like Fermi surface (FS) around the M point as illustrated in Fig. 1. In the following we discuss how spin-fluctuation scattering involving intermediate virtual states of the incipient band can lead to an effective retarded pairing interaction for the electrons on the electron Fermi surface.

Various authors have suggested that an $s^{\pm}$ pairing state can be formed in which a gap appears on the incipient band with the opposite sign to the gap on the electron Fermi surface [10–12]. Here using a dynamic cluster approximation (DCA) [13] quantum Monte Carlo (QMC) calculation for a bilayer Hubbard model we show that this physics can be described in terms of an effective pairing interaction for the fermions near the electron Fermi surface. Unlike the usual momentum dependent spin-fluctuation pairing interaction, this effective interaction is essentially independent of momentum transfer, but depends upon the Matsubara frequency transfer. It is local in space but retarded in time. While the resulting superconducting state is similar to that of the incipient band pairing proposals, the introduction of an effective interaction provides a different perspective on the pairing interaction. In this case, just as in the traditional electron-phonon superconductors, it is the frequency dependence of the pairing interaction rather than its momentum dependence that is important. As a consequence, it is the sign change of the gap with frequency that characterizes the pairing.

The system we will study is a bilayer Hubbard model with

$$H = t \sum_{\langle ij\rangle m\sigma} (c^{\dagger}_{im\sigma} c_{jm\sigma} + \text{h.c.}) + t_{\perp} \sum_{i\sigma} (c^{\dagger}_{i1\sigma} c_{i2\sigma} + \text{h.c.}) - \mu \sum_{im\sigma} n_{im\sigma} + U \sum_{im} n_{im\uparrow} n_{im\downarrow} \,. \quad (1)$$

The operator $c^{\dagger}_{im\sigma}$ creates an electron on the i^{th} site of the $m = 1$ or 2 layer with spin σ and $n_{im\sigma} = c^{\dagger}_{im\sigma} c_{im\sigma}$. Here t is the intra-layer near neighbor hopping, $t_{\perp}$ the inter-layer hopping and U the on site interband Coulomb interaction. The bandstructure for periodic boundary conditions is

$$\varepsilon_{\boldsymbol{k}} = 2t(\cos k_x + \cos k_y) + t_{\perp} \cos k_z - \mu \,. \quad (2)$$

In this model $t_{\perp}$ sets the energy separation between the bonding and antibonding bands rather than the orbital energies which are expected to play this role in the actual materials. Similarly, in this model, $t_{\perp}$ is important in determining the strength and momentum dependence of the spin fluctuations. Our goal in this paper is to carry out detailed numerical calculations for a simple model which has an incipient band and examine the structure of the effective pairing interaction which can arise in such a system.

The results which will be shown are obtained from a DCA calculation on a $(4 \times 4) \times 2$ cluster with 16 sites in each layer. In the DCA, the momentum space is coarse-grained and thereby the lattice problem is reduced to a finite size cluster embedded in a mean-field that is self-consistently determined to represent the remaining lattice degrees of freedom [13]. This 32-site cluster problem is then solved with a continuous-time auxiliary-field QMC algorithm [14, 15]. While the $\boldsymbol{k}$ dependence of irreducible quantitites, i.e. the single-particle self-energy and

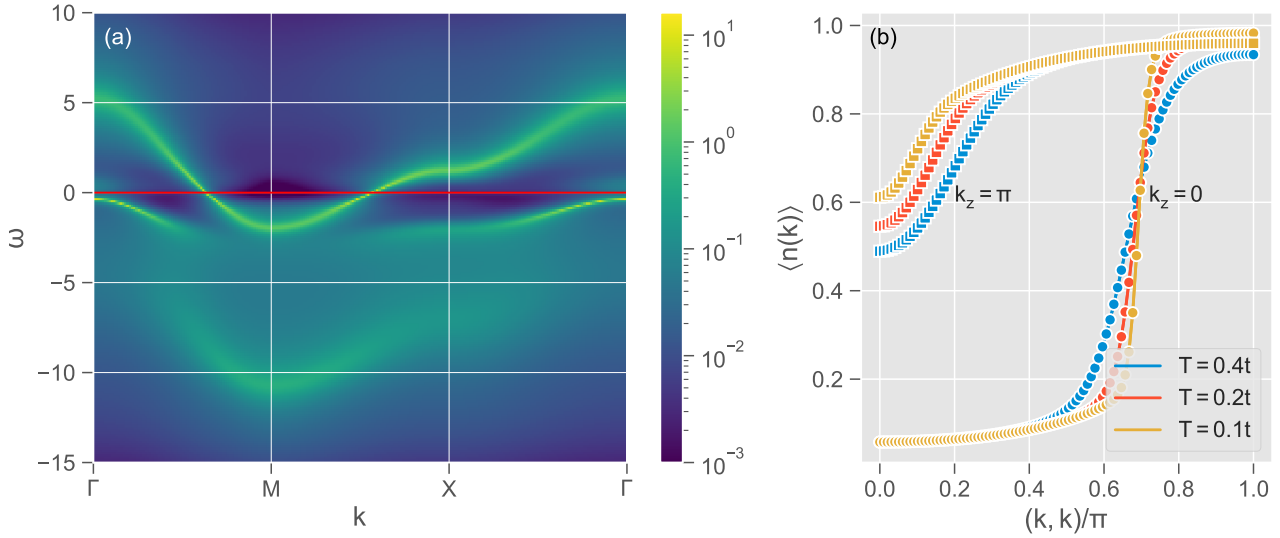

FIG. 1: (a) The single particle spectral weight $A(\boldsymbol{k},\omega)$ at $T = 0.2$ for $t_\perp = 2.5$, $n = 1.15$ and $U = 8$ shows an electron pocket around the $(k_x = \pi,\ k_y = \pi)$ M point for $k_z = 0$ and an incipient hole band laying below the Fermi energy and centered at the $(k_x = 0,\ k_y = 0)$ Γ point for $k_z = \pi$. (b) The momentum occupation $\langle n(\boldsymbol{k})\rangle$ plotted for $\boldsymbol{k}$ running from Γ to M sharpens at the electron FS as the temperature is decreased, and is suppressed at Γ as the $k_z = \pi$ band drops below the Fermi energy.

the irreducible two-particle vertex functions, is reduced to the 32 cluster momenta, the full lattice $\boldsymbol{k}$-dependence is retained in the Green's function through the dispersion Eq. (2) [13]. In this approximation, correlations within a length-scale set by the cluster size are treated accurately by QMC, while longer-ranged correlations beyond the cluster are treated at a mean-field level.

In the following we will set $t_\perp/t = 2.5$, $U/t = 8$ and take a filling $n = 1.15$. For these parameters, the single-particle spectral weight $A(\boldsymbol{k},\omega)$, obtained from a Maximum Entropy estimation, plotted in Fig. 1(a), shows evidence of a $k_z = 0$ electron Fermi surface around the $(k_x = \pi,\ k_y = \pi)$ M point and an incipient $k_z = \pi$ hole band that has dropped just below the Fermi energy at the Γ point. Consistent with this, the momentum distribution $\langle n(\boldsymbol{k})\rangle$ for $k_z = 0$ shown in Fig. 1(b) sharpens at $\boldsymbol{k}_F$ as the temperature is reduced, while for $k_z = \pi$, $\langle n(\boldsymbol{k})\rangle$ fades away as T decreases indicating that the $k_z = \pi$ band lays below the Fermi energy. Further evidence of an incipient $k_z = \pi$ band is seen in the behavior of the intrinsic pairfield susceptibility

$$P^0_{k_z}(T) = \frac{T}{N}\sum_{k,\omega_n} \phi^2(\omega_n) G_{k_z}(\boldsymbol{k},\omega_n) G_{k_z}(-\boldsymbol{k},-\omega_n) \quad (3)$$

Here we have used a smooth frequency cut-off $\phi(\omega_n) = (\pi^2T^2 + \omega_c^2)/(\omega_n^2 + \omega_c^2)$ with $\omega_c = t$. $G_{k_z}(\boldsymbol{k},\omega_n)$ is the dressed single particle propagator associated with the $k_z = 0$ or π bands, $\boldsymbol{k} = (k_x, k_y)$ and $\omega_n = (2n+1)\pi T$ is a Matsubara frequency. The intrinsic pairfield susceptibility is expected to exhibit a Cooper $\log(t/T)$ behavior when there is a Fermi surface. As shown in Fig. 2, one sees this type of behavior for the $k_z = 0$ electrons, but $P^0_\pi(T)$ for the $k_z = \pi$ hole band remains flat as T decreases.

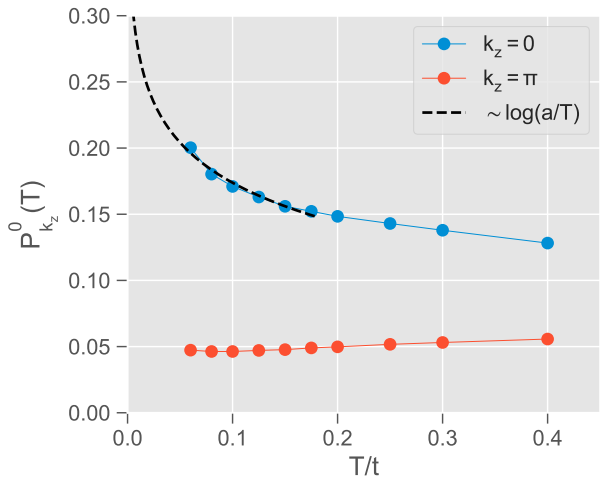

FIG. 2: The intrinsic pairfield susceptibilities $P^0_0(T)$ and $P^0_\pi(T)$ versus T. $P^0_0(T)$ exhibits a $\log(t/T)$ Cooper instability associated with the $k_z = 0$ Fermi surface while $P^0_\pi(T)$ for the incipient band remains flat as T decreases.

With this in mind, we consider the pairing interaction $\Gamma(K,K')$ with $K = (k_x, k_y, i\omega_n)$ and $K' = (k'_x, k'_y, i\omega_{n'})$ between fermion pairs near the $k_z = 0$ electron FS. This interaction can be separated into two particle-particle scattering vertices

$$\Gamma(K,K') = \Gamma_1(K,K') + \Gamma_2(K,K')\,. \quad (4)$$

The first of these, Γ_1, involves intermediate pair scattering processes near the electron Fermi surface ($k_z = 0$) while $\Gamma_2(K,K')$ involves the incipient ($k_z = \pi$) hole band. A schematic illustration of $\Gamma_2(K,K')$ is shown

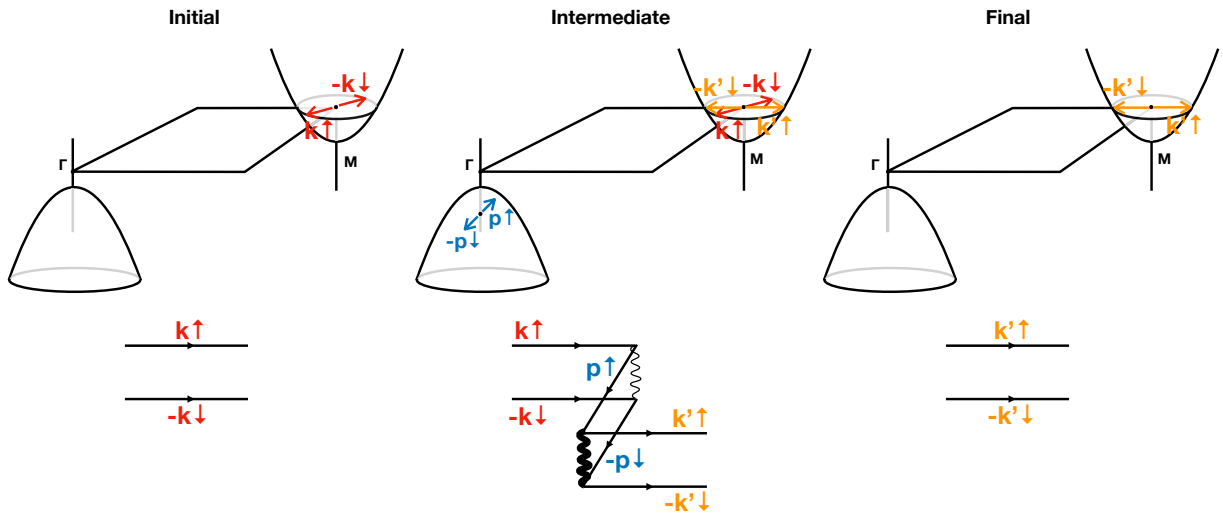

FIG. 3: Schematic illustration of the effective intermediate state contribution to the Γ_2 pairing vertex. The Feynman diagram for Γ_2 shown in the lower part of the figure involves the intermediate states illustrated above it. The thin interaction line denotes the $\Gamma^0_{0\pi}$ fully irreducible vertex and the thicker interaction line the $\Gamma_{\pi 0}$ vertex, which is only irreducible in the $k_z = 0$ two-particle channel.

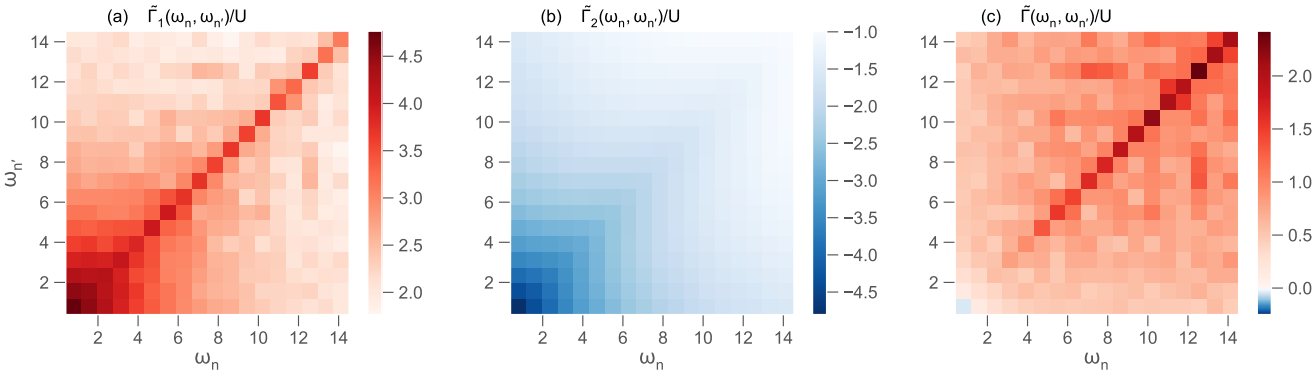

FIG. 4: The two particle scattering vertices for $T = 0.125t$, normalized to U, versus the Matsubara energies ω_n and $\omega_{n'}$. (a) $\tilde{\Gamma}_1(\omega_n, \omega_{n'})$, (b) $\tilde{\Gamma}_2(\omega_n, \omega_{n'})$ and (c) their sum $\tilde{\Gamma}(\omega_n, \omega_{n'})$.

in Fig. 3. Here, as seen in Fig. 3, the low energy physics of this model that determines the effective pairing interaction $\Gamma(K, K')$ involves the virtual excitation of pairs to and from the incipient band. The momentum structure of the effective interaction is weak because it involves a range of states on the incipient band rather than being dominated by states near the Fermi surface as in the usual Fe-based superconducting case where there are both electron and hole pockets.

Γ_1 is irreducible in both the $k_z = 0$ and $k_z = \pi$ particle-particle channels while Γ_2 is irreducible in only the $k_z = 0$ channel. As shown in the Feynman diagram in Fig. 3, Γ_2 can be written as

$$\Gamma_2(K, K') = -\frac{T}{N} \sum_{K''} \Gamma^0_{0\pi}(K, K'') G_\pi(K'') G_\pi(-K'') \times \Gamma_{\pi 0}(K'', K') \,. \quad (5)$$

Here the $\Gamma^0_{0\pi}$ vertex involves pairs with $k_z = 0$ near the electron FS which scatters to states in the incipient $k_z = \pi$ band. It is irreducible in both the $k_z = 0$ and π two particle channels. The single particle Green's function $G_\pi(K'')$ is the dressed electron propagator on the incipient band and the vertex $\Gamma_{\pi 0}$ is only irreducible in the $k_z = 0$ channel, so that Γ_2 contains multiple scattering processes involving pairs on the incipient $k_z = \pi$ band.

The important momentum dependence of the pairing interaction which involves the inter-band $k_z - k'_z = \pi$ scattering has been separated out and the Γ vertices in Eq. (4) are slowly varying functions of $k_x - k'_x$ and $k_y - k'_y$. The important variables are the Matsubara energies ω_n

and $\omega_{n'}$. The gap is an even function of ω_n so that it is useful for plotting to introduce symmetrized vertices [16]

$$\tilde{\Gamma}(\omega_n, \omega_{n'}) = \Gamma(\omega_n, \omega_{n'}) + \Gamma(\omega_n, -\omega_{n'}) \quad (6)$$

with ω_n and $\omega_{n'}$ varying over positive Matsubara frequencies. Results for $\tilde{\Gamma}_1(\omega_n, \omega_{n'})$ and $\tilde{\Gamma}_2(\omega_n, \omega_{n'})$ are plotted in Fig. 4 (a-b) for $\boldsymbol{k}$ and $\boldsymbol{k}'$ set to (π, π). The contribution to the pairing interaction from pair scatterings on the FS, $\tilde{\Gamma}_1(\omega_n, \omega_{n'})$, is positive while the contribution from the virtual pair scattering involving the $k_z = \pi$ band, $\tilde{\Gamma}_2(\omega_n, \omega_{n'})$, is negative. The strength of the attractive $\tilde{\Gamma}_2$ is associated with the spin-fluctuation $k'_z - k_z = \pi$ scattering processes that scatter pairs between the electron Fermi surface and the incipient band. It is this transfer rather than the scattering interactions on the incipient band that is important. The $\omega_{n'} = \omega_n$ cleft in $\tilde{\Gamma}_2(\omega_n, \omega_{n'})$ shown in Fig. 4 (b) corresponds to having zero center of mass energy in this transfer process.Combining Γ_1 and Γ_2, the resulting effective pairing interaction Γ plotted in Fig. 4c is positive (repulsive) everywhere except for the lowest frequency where it is negative (attractive).

Solving the Bethe-Salpeter equation

$$-\frac{T}{N}\sum_{K'} \Gamma(K, K')G_\pi(K')G_\pi(-K')\phi(K') = \lambda\phi(K) \quad (7)$$

with $K = (k_x, k_y, \omega_n)$, we find the leading eigenvalue λ_0 and eigenfunction $\phi_0(\boldsymbol{k}, \omega_n)$ shown in Fig. 5. As noted, the irreducible vertex $\Gamma(K, K')$, and therefore the eigenfunction $\phi_0(K)$ only depend on the 32 DCA cluster momenta, while the Green's function $G(K)$ retains the full momentum dependence of the lattice [17]. The eigenfunction $\phi_0(\boldsymbol{k}, \omega_n)$ is essentially independent of $\boldsymbol{k}$ as shown in Fig. 5b but, as shown in Fig. 5c changes sign as ω_n increases. This sign change is such that the gap function is positive over the frequency regime characteristic of the spin-fluctuations plus the depth of the incipient band below the Fermi energy. Since the interaction Γ increases with frequency and the sign of $\phi(\boldsymbol{k}, \omega_n)$ changes with frequency, the Bethe-Salpeter equation (7) can be satisfied with a positive λ although Γ is positive over most of the frequency range. This is similar to the frequency dependence of the gap in the traditional electron-phonon-Coulomb problem. There the eigenfunction $\phi(\boldsymbol{k}, \omega_n)$ is positive when $|\omega_n|$ is less than several times the typical phonon energy and changes sign at larger frequencies leading to a suppression of the Coulomb repulsion.

To summarize, in this picture (1) antiferromagnetic order is suppressed as the hole (or electron) band becomes incipient, leaving strong $k'_z - k_z = \pi$ spin-fluctuations, (2) the pairing interaction arises from spin fluctuation scattering processes which involve intermediate states on the incipient band and give rise to an attractive retarded pairing interaction for the fermions on the remaining electron Fermi surface, and (3) the resulting gap function has

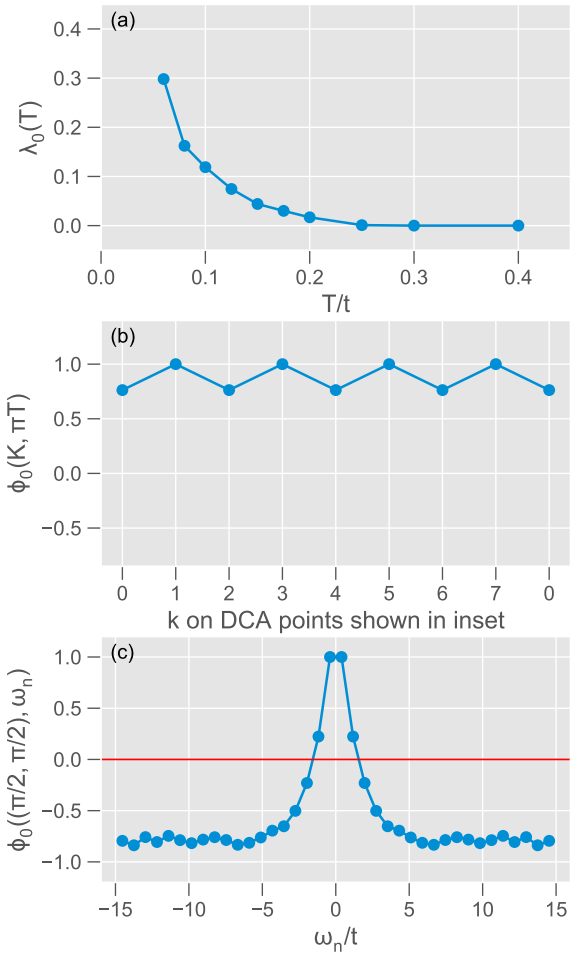

FIG. 5: (a) The leading eigenvalue $\lambda_0(T)$ of the Bethe-Salpeter equation as T decreases. (b) The momentum dependence of the gap function $\phi_0(\boldsymbol{k}, \omega_n)$ of the leading eigenvalue for $\omega_0 = \pi T$ for $\boldsymbol{k}$ values near the FS as shown in the inset and (c) its frequency dependence for $\boldsymbol{k} = (\pi/2, \pi/2)$ for $T = 0.125t$. $\phi_0(\boldsymbol{k}, \omega_n)$ changes sign leading to a reduction of the effect of the repulsive Γ_1 interaction.

A_{1g} symmetry with a weak k-dependence, but changes sign as a function of $|\omega_n|$. This change in sign is a significant feature and should be observable in tunneling experiments. Finally, the occurrence of this type of effective pairing interaction, which arises from the virtual scattering of pairs to and from an incipient band, should be more general both with respect to the nature of the primary interaction as well as the band structure of the separate layers.

Acknowledgments

This work was supported by the Scientific Discovery through Advanced Computing (SciDAC) program funded by the U.S. Department of Energy, Office of Sci-

ence, Advanced Scientific Computing Research and Basic Energy Sciences, Division of Materials Sciences and Engineering. An award of computer time was provided by the INCITE program. This research used resources of the Oak Ridge Leadership Computing Facility, which is a DOE Office of Science User Facility supported under Contract DE-AC05-00OR22725.

[1] I.I. Mazin, *Nature Materials* **14**, 755 (2015)

[2] Q.-Y. Wang, Z. Li, W.-H. Zhang, Z.-C. Zhang, J.-S. Zhang, W. Li, H. Ding, Y.-B. Ou, P. Deng, K. Chang, J. Wen, C.-L. Song, K. He, J.-F. Jia, S.-H. Ji, Y.-Y. Wang, L.-L. Wang, X. Chen, X.-C. Ma, and Q.-K. Xue, Chin, *Phys. Lett.* **29**, 037402 (2012).

[3] D. F. Liu, W. H. Zhang, D. X. Mou, J. F. He, Y.-B. Ou, Q.-Y. Wang, Z. Li, L. L. Wang, L. Zhao, S. L. He, Y. Y. Peng, X. Liu, C. Y. Chen, L. Yu, G. D. Liu, X. L. Dong, J. Zhang, C. T. Chen, Z. Y. Xu, J. P. Hu, X. Chen, X. C. Ma, Q. K. Xue, and X. J. Zhou, *Nat. Comm.* **3**, 931 (2012).

[4] S.L. He, J. F. He, W. H. Zhang, L. Zhao, D. F. Liu, X. Liu, D. X. Mou, Y.-B. Ou, Q.-Y. Wang, Z. Li, L. L. Wang, Y. Y. Peng, Y. Liu, C. Y. Chen, L. Yu, G. D. Liu, X. L. Dong, J. Zhang, C. T. Chen, Z. Y. Xu, X. Chen, X. C. Ma, Q. K. Xue, and X. J. Zhou, *Nat. Mater.* **12**, 605 (2013).

[5] J. F. Ge, Z. L. Liu, C. H. Liu, C. L. Gao, D. Qian, Q. K. Xue, Y. Liu, and J. F. Jia, *Nat. Mater.* **14**, 285 (2015).

[6] X. F. Lu, N. Z. Wang, G. H. Zhang, X. G. Luo, Z. M. Ma, B. Lei, F. Q., Huang, and X. H. Chen *Phys. Rev. B* **89**, 020507(R) (2014).

[7] Y. Miyata, K. Nakayama, K. Sugawara, T. Sato and T. Takahashi, *Nat. Mater.* **14**, 775 (2015).

[8] X. H. Niu, R. Peng, H. C. Xu, Y. J. Yan, J. Jiang, D. F. Xu, T. L. Yu, Q. Song, Z. C. Huang, Y. X. Wang, B. P. Xie, X. F. Lu, N. Z. Wang, X. H. Chen, Z. Sun, and D. L. Feng, *Phys. Rev.* B **92**, 060504(R) (2015).

[9] Y. J. Yan, W. H. Zhang, M. Q. Ren, X. Liu, X. F. Lu, N. Z. Wang, X. H. Niu, Q. Fan, J. Miao, R. Tao, B. P. Xie, X. H. Chen, T. Zhang, and D. L. Feng, *Phys. Rev. B* **94**, 134502 (2016)

[10] Xiao Chen, S. Maiti, A. Linscheid, and P. J. Hirschfeld, *Phys. Rev. B* **92**, 224514 (2015).

[11] A. Linscheid, S. Maiti, Y. Wang, S. Johnston, and P. J. Hirschfeld, *Phys, Rev. Lett.* **117**, 077003 (2016)

[12] V. Mishra, D. J. Scalapino, T. A. Maier, *Scientific Reports* **6**, Article number: 32078 (2016)

[13] T. Maier, M. Jarrell, T. Pruschke, and M. Hettler, *Rev. Mod. Phys.* **77**, 1027 (2005).

[14] E. Gull, P. Werner, O. Parcollet, and M. Troyer, *Europhys. Lett.* **82**, 57003 (2008).

[15] E. Gull, P. Staar, S. Fuchs, P. Nukala, M. Summers, T. Pruschke, T. Schulthess, and T. Maier, *Phys. Rev. B* **83**, 075122 (2011).

[16] While it is convenient to plot the ω_n and $\omega_{n'}$ dependence of the symmetrized vertex $\tilde{\Gamma}$, as shown in Fig. 4, in the Bethe-Salpeter equation (7) we have used the unsymmetrized vertex so that in principle one could have odd-frequency p-wave singlet and s-wave triplet solutions. We find that the even frequency s-wave singlet has the leading eigenvalue for temperatures $T \lesssim 0.15t$.

[17] T. A. Maier, M. S. Jarrell, and D. J. Scalapino, *Phys. Rev. Lett.* **96**, 047005 (2006).